DOI 10.1007/s11595-014-0932-5

Effect of Coated PHB on Properties of Abradable Seal Coating

CHENG Xudong[1], XIANG Hongyu[1,2], YE Weiping[2], MENG Xiaoming[2], MIN Jie[1], LIU Minzhi[1], ZHANG Pu[1], LU Wei[1]

(1.State Key Laboratory of Advanced Technology for Materials Synthesis and Processing, Wuhan University of Technology, Wuhan 430070, China; 2.College of Materials Science and Engineering, Wuhan University of Technology, Wuhan 430070, China)

Abstract: As pore-forming materials, the coated poly-p-hydroxybenzoate(short for PHB) and h-BN can be applied in the preparation of abradable seal coatings at high temperature. The characteristics of coating such as morphology, thermal stability and composition were studied by SEM, EDS and FTIR. The results show that the modified PHB will change the remained carbon amount, porosity and pore morphology of the coating, which can affect the properties of coatings. If the pore is small enough in uniform distribution, the coating with 5 MPa bond strength, 30-55 HR45Y superficial hardness and certain of carbon can be suitable to well abradability.

Key words: coated-PHB; pore morphology; seal coating

1 Introduction

From the aspects of higher operating temperature and low clearance between engine blades and inner wall of engine, the efficiency of gas turbine systems can be enhanced, which depends on a well abradable seal coating (ASC)[1]. Among whole loss of energy in the aircraft engine, the leakage gas of the blades tip accounts for 10%-40%. However, if the clearance is reduced around 0.13-0.25 mm, the efficiency of engine is increased by around 2% and the oil consumption can be reduced by 0.5%-1%[2]. The porous honeycombed structure can contribute to adjust the hardness and bond strength at high temperature[4]. Based on burning off and carbonization in the process of atmospheric plasma spraying (APS), polymer such as PHB scarcely deposits on coatings, resulting in low porosity[5]. In this paper, the alumina sol and zirconia sol were applied to prepare the surface modified PHB for higher decomposition temperature. The coated PHB was encompassed by semi-vitreous alumina or zirconia to avoid contacting with flame directly in high temperature burning flow.

(Received: Oct. 27, 2013; Accepted: Jan. 25, 2014)

CHENG Xudong(程旭东): Prof.; E-mail: xudong.cheng@whut.edu.cn

Funded by the Foundation of State Key Laboratory of Advanced Technology for Materials Synthesis and Processing

2 Experimental

2.1 Preparation of seal powder

The agglomerated powder components and performances are listed in Table 1. There were nano ZrO_2-8 wt% Y_2O_3(20-60 nm, short for YPSZ), nano-Al_2O_3(15-30 nm), micron-sized h-BN(0.25-2 μm) and coated PHB as raw powders respectively. The abbreviation of laboratory-prepared powders and coating is listed in Table 2. The ACP and ZCP were prepared when alumina sol and zirconia sol were mixed with decomposition of PHB under magnetic stirring at 60-70 ℃. After drying, cooling, milling and sieving, the particles of diameter between 50 and 150 μm were suitable to the raw powders. The as-received YPSZ, Al_2O_3, h-BN, coated PHB powders were dispersed by ultrasonic dispersion in ethanol for 20 min. Slurry which was acquired by raw powders and deionized water in proportion was ground well in colloid mill. The agglomerated powders were fabricated by spray drying in the spray dry tower at a 250-300 ℃ air intake temperature and a 30-50 ℃ outlet temperature. After cooling in air, the agglomerated powders were passed through a 125 μm sieve before being plasma sprayed. Flowability and apparent density of agglomerated particles were investigated by FL4-1 hall flow meter.

2.2 Atmospheric plasma spraying

The specimens were made by 06Cr18Ni10Ti

Table 1 Agglomerated powders components and performance

Powder	Composition/%				Apparent density/(g · cm^{-3})	Flowability /(s · 50 g^{-1})
	YPSZ	Detached Al_2O_3	h-BN	PHB and state		
A	83	10	2	5(uncoated)	2.84	1.1
B	83	9.12	2	5.88(Al_2O_3 coated PHB)	2.88	1.1
C	81.33	10	2	6.67 (ZrO_2 coated PHB)	2.81	0.95

Table 2 Laboratory-prepared powders and coating

Abbreviation	Description
ACP	Al_2O_3-coated PHB
ZCP	ZrO_2-coated PHB
C1	As-sprayed coating by agglomerated powder A
C2	As-sprayed coating by agglomerated powder B
C3	As-sprayed coating by agglomerated powder C

stainless steel in the size of *Φ*40 mm×8 mm, which were cleaned by ultrasonic for 20-30 min, and sandblasted by corundum. Three different kinds of agglomerated powders and NiCrAlY powders were sprayed through GP-80 plasma spraying equipment with inner and outer feedstock respectively that deposited on specimens. The thickness of the bond coating was about 100 μm and the top coating was 1 500-2 000 μm. In order to obtain the coatings with well bond strength, the optimized spray parameters[6] are listed in Table 3.

2.3 Characterization

Thermal gravimetry with differential scanning calorimetry(TG-DSC) of the coated PHB was conducted by a scanning calorimeter(NETZSCH, STA449c/3/G, Germany). The temperature program in the experiment rose from 30 to 1 000 ℃ at the speed of 5 ℃/min in air flow[7]. The samples were sectioned and polished to study the cross-sectional microstructure by SEM analysis (JSM-5610LV, Japan). The functional groups were identified by Fourier transform infrared spectroscopy (Nexus, Thermo Nicolet, USA) at 4 000-400 cm^{-1}(2.5-25 μm) intermediate infrared. Superficial hardness and bond strength were examined using superficial rockwell hardness tester (TH310, TME, USA) and hydraulic universal tester (WE-100A, China).

3 Results and discussion

3.1 Characteristics of coated PHB

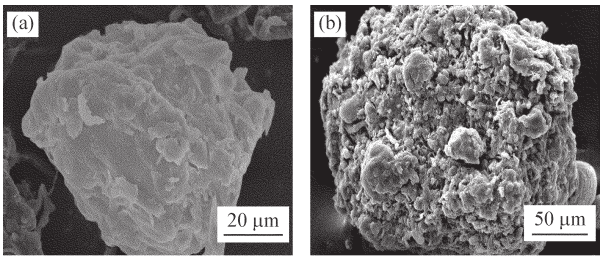

(a) ACP (b) ZCP

Fig.1 SEM images of coated PHB

Fig.1 shows scanning electron micrographs of ACP and ZCP. The performance of PHB depends on particle size, dispersity and morphology[3], which is used as poreforing material in the seal coating. But actually, most part of PHB is burned off in the process of APS, resulting in the low porosity of coating[8].

In our pretreatment, alumina sol and zirconia sol were employed as core-shell because of its high melting point and easy preparation. The porous performance of coated PHB depends on the coated integrality and thermal protection of core-shell[9]. In coating process, ACP was prepared by heterogeneous nucleation process between the hydrolyzate of aluminium isopropoxide and dispersed PHB, which generated chain-growth product. This method can be adopted in the fabrication of ZCP by zirconium oxychloride and dispersed PHB. From Fig.1, it can be seen that both ACP and ZCP illustrate irregular ball-like morphology with bump particles. Especially, compared with the size of ACP ranging from 50 to 100 μm in diameter, ZCP was made in larger size ranging from 100 to 150 μm, to identify

Table 3 Spraying process parameters

Parameter	Current/A	Voltage/V	Primary gas flow rate (Ar+N_2) /(m^3 · h^{-1})	Secondary gas flow rate (H_2) /(m^3 · h^{-1})	Powder feed rate /(g · min^{-1})	Spraying distance /mm
Bond coating	75	450	2.0	-	40	120-125
Top coating	80	500	1.8	0.2	30	80-85

the connection between the thickness of core-shell and property of coating.

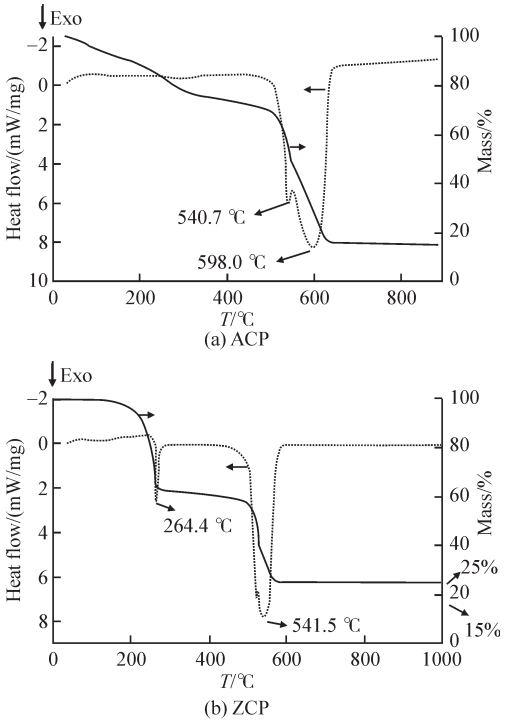

Fig.2 TG-DSC curves of coated powders

In addition, the TG-DSC analysis results of two coated powders are shown in Fig.2.Their oxidative and thermal behaviors are comparable. The TG-DSC curves of PHB show single mass loss between 250 and 400 ℃[10,11] with different heating rates. The TG curve of ACP shows in both cases a relatively slight mass loss between 30 and 300 ℃, followed by a second strong loss between 500 and 650 ℃. These mass variations are related to adsorbed water and constituent water, the latter confirms combustion and complete volatilization of the chain-growth product.

At the same time, the DSC curve of ACP presents two exothermic peaks at approximately 540 and 600 ℃, related to the oxidative decompositions. Besides, approximate 15% of chain-growth product can resist the high temperature below 1 000 ℃ due to the core-shell Al_2O_3. The homologous and more obvious curves can be found in the TG-DSC curves of ZCP, resulting from larger size previously mentioned. The TG of ZCP shows a mass loss between 100 and 300 ℃, followed by a second loss between 500 and 650 ℃, which relates to constituent water and combustion of PHB. In both coated-PHB, there are relative 15% and 25% of powders resisted below 1 000 ℃ due to alumina and zirconia. These findings suggest that coated PHB can be improved regarding the oxidative decomposition point, averagely ranging from 300 to 550 ℃, compared with uncoated PHB.

3.2 Organic matter in coating

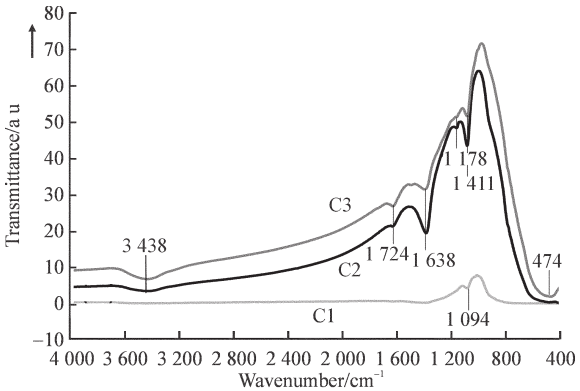

Fig.3 FTIR spectra of C1,C2,C3

Three FTIR spectra of the coatings fabricated by agglomerated powders are shown in Fig.3. The spectra of C2 and C3 reveal absorption peak at 3 438 cm^{-1} for －OH stretching vibration in the carboxyl group indicating the presence of structured water[13] and absorption peaks at 1 724, 1 638, 1 178, 1 411 cm^{-1} for －C＝O, －C＝C－, －C－O－, $-CH_3$ stretching vibrations in esters and benzene respectively. Differently, an single absorption band around 1 034 cm^{-1} is observed due to －C＝O－ stretching vibration[10] in the spectrum of C1 and a broad band around 474 cm^{-1}[14] corresponds to Zr－O vibration in the spectrum of C3. The functional groups of PHB(－C＝C－, －C＝O, －C－O－,$-CH_3$) can be observed in C2 and C3 which suggest that the remaining degradation of PHB existed in coating, compared with the single －C－O－ stretching vibration in C1. Katharina Richardt's research found that more polyester would burn off during the spray process, consequently causing less polyester to be deposited on the as-sprayed coating[13]. Indeed, from the spectrum of C1, it can be seen that mass of PHB was burning loss without alumina or zirconia protection in the process of APS. But with the core-shell, different structure of PHB can be observed in coatings.

3.3 Morphology and mechanic properties

The images of fractured cross-section morphology of the as-sprayed coatings with polishing made by secondary electronic imaging technology are shown in Fig.4. Fig.4(a) and Fig.4(b) display the micro morphology of C1 and C2 respectively. Fig.4(c)-4(f) display the different micro structures of C3. The APS coatings show typical microstructure with dense area (melted particles and nano sized grains)[12], cellular

structure(partially melted or unmelted particles), splats, globular pores and vertical or transverse cracks. For obtaining the distribution of carbon content, EDS element mapping results of C3 are presented in Fig.5.

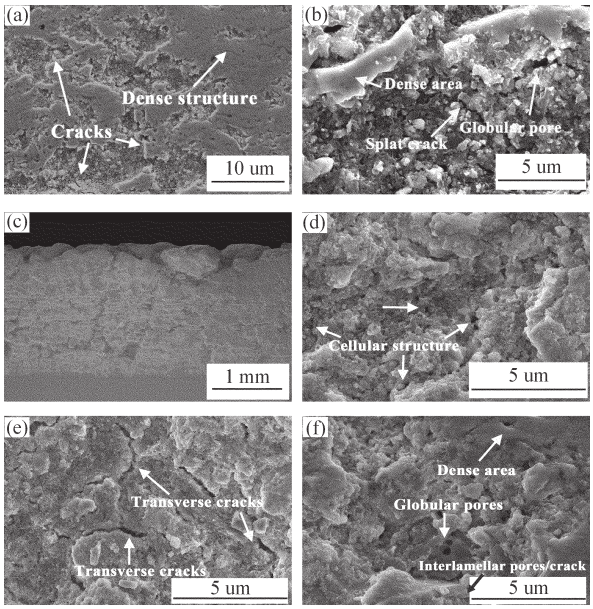

Fig.4 SEM images of the polished cross-section: (a) C1; (b) C2; (c),(d),(e),(f) C3

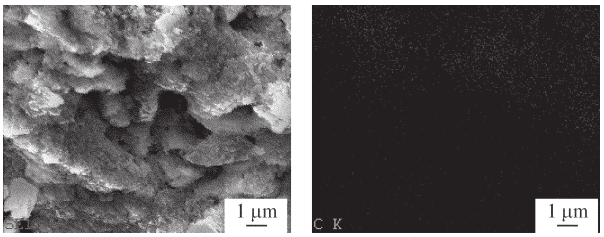

Fig.5 EDS elemental mapping of the C from the cross section of C3

Table 4 Mechanical properties

Coating	Thickness /mm	Porosity /%	Hardness /R45y	Bond strength /MPa(>)
C1	1.88	5.3	65.9	9.0
C2	1.98	9.2	45.4	7.4
C3	1.95	11.2	42.7	7.2

Archimedes displacement water principle and suspension method were employed to measure the porosity of coating. Superficial hardness and bond strength were tested by durometer and universal testing machine and the result is shown in Table.4. This test relied on a bonding agent to remove the coating from metal substrate with longitudinal force. The value of the bonding strength can be collected from the spalling force over the stressed area.

It can be seen from Fig.4(a) that dense structure and low porosity can be found, which show the same as conventional ASC. It has been verified that the abrasion resistance of thermal sprayed coating is related to the relative fracture toughness[16-18]. Fig.4(b) presents that uniform and abundant pores were observed around unmelted particles, splat crack was comprised of many successional pores and dense area was smooth. Based on the mechanism of micro-crack toughness[19], the more splat cracks and micro cracks, the more stress of crack propagating can be avoided. The nano-structured as-sprayed ZrO_2 presented well fracture toughness. Besides, the particle boundaries between ZrO_2 and Al_2O_3 grains improved the micro crack resistance and enhanced the fracture toughness[15]. The uniform and abundant micro pores caused a loosened cellular structure. Figs.4(c)-4(f) present the typical cellular structure, vertical or transverse cracks, globular pores and interlamellar pores or cracks respectively, which show well compositive property. The surface hardness of C3 is around 42.7HR45Y which is lower than conventional ASC. The dense area is composed of melted grains[12] while the loose celluar structure contains the equiaxial grains and nanosized grains. This characteristic of the microstructure is beneficial to enhance the wear resistance of ASC. With the surface modified PHB addition, the porosity of coating increased significantly from 5.3% (65.9HR45Y) to 11.2% (42.7HR45Y) with the required bond strength (above 5 MPa). There are two kinds of pores in coating. One is formed by nano sized grains in the process of APS which is observed between boundaries with diminutive size (about 0.1 μm) and irregular inwall. The other one is fabricated by ablating carbide in the process of thermal cycle which is observed in the dense area with relative globular size (about 0.5 μm) and smooth inwall. The superficial Hardness can be correlated with the porosity[13], suggesting that higher porosity leads to a lower coating hardness. But higher porosity leads to low bond strength for the loosened structure of the coating.

4 Conclusions

Both ACP and ZCP were fabricated by heterogeneous nucleation process to modify the surface of PHB. Alumina and zirconia were agglomerated in the way of detached nano powders and coated state with coated PHB, which were used to make abradable seal coatings on the stainless steel surface. The coatings with the addition of coated PHB have well abradable properties, which display the better properties, such

as higher porosity, lower surface hardness and bond strength.

The integrated functional group of PHB can be observed in the as-sprayed coatings with coated PHB. There is the great effect on the micro morphology, such as distributing uniform pores, less dense area and abundant micro cracks to make the cellular structure. The hardness and bond strength reveal that the average hardness is HR45Y 42.7 which is lower than that of conventional abradable coatings and the average bond strength is 7.2 MPa which meets the requirement.

References

[1] S Ahmaniemi, P Vuoristo, T Mantyla. Improved Sealing Treatments for Thick Thermal Barrier Coatings[J]. *Surface and Coatings Technology*, 2002,151-152: 412-417

[2] H I Faraoun, J L Seichepinea, C Coddeta, *et al.* Modelling Route for Abradable Coatings[J]. *Surface & Coatings Technology*, 2006, 200: 6 578-6 582

[3] Yoshio Akimune, Kazuo Matsuo, Satoshi Sodeoka, *et al.* Point Load-induced Fracture Behavior in Zirconia Plasma Spray Coating[J]. *Ceramics International*, 2004, 30: 2 251-2 257

[4] Wei-Jen Shih, Yi-Hung Chen, Chi-Jen Shih, *et al.* Structural and Morphological Studies on Poly(3-hydroxybutyrate acid) (PHB)/ Chitosan Drug Releasing Microspheres Prepared by both Single and Double Emulsion Processes[J]. *Journal of Alloys and Compounds*, 2007, 434-435: 826-829

[5] M L Sanjuán, P B Oliete, A Várez, *et al.* The Role of Ce Reduction in the Segregation of Metastable Phases in the ZrO_2–CeO_2 System[J]. *Journal of the European Ceramic Society*, 2012, 32: 689-696

[6] R E Johnston. The Sensitivity of Abradable Coating Residual Stresses to Varying Material Properties[J]. *Journal of Thermal Spray Technology*, 2009, 18(5-6): 1 004-1 013

[7] Pyung-Ho Lee, Sang-Yup Lee, Jae-Young Kwon, *et al.* Thermal Cycling Behavior and Interfacial Stability in Thick Thermal Barrier Coatings[J]. *Surface & Coatings Technology*, 2010, 205: 1 250-1 255

[8] B Liang, G Zhang, H L Liao, *et al.* Structure and Tribological Performance of Nanostructured ZrO_2-3 mol% Y_2O_3 Coatings Deposited by Air Plasma Spraying[J]. *Journal of Thermal Spray Technology*, 2010, 19(6): 1 163-1 170

[9] J Chandradass, M Balasubramanian. Sol-gel Processing of Alumina-Zirconia Minispheres[J]. *Ceramics International*, 2005, 31: 743-748

[10] Si-Dong Li, Ji-Dong He, Peter H Yu, *et al.* Thermal Degradation of Poly(3-hydroxybutyrate) and Poly(3-hydroxybutyrate-co-3-hydroxyvalerate) as Studied by TG, TG–FTIR, and Py–GC/MS[J]. *Iranian Polymer Journal*, 2011, 20(5): 423-432

[11] A C Karaoglanli, E Altuncu, I Ozdemira, *et al.* Structure and Durability Evaluation of YSZ+Al_2O_3 Composite TBCs with APS and HVOF Bond Coats under Thermal Cycling Conditions[J]. *Surface & Coatings Technology*, 2011, 205: S369-S373

[12] Qinghe Yu, Abdul Rauf, Chungen Zhou. Microstructure and Thermal Properties of Nanostructured 4 wt%Al_2O_3-YSZ Coatings Produced by Atmospheric Plasma Spraying[J]. *Journal of Thermal Spray Technology*, 2010,19(6): 1 294-1 300

[13] Katharina Richardt, Kirsten Bobzin, Dieter Sporer, *et al.* Tailor-Made Coatings for Turbine Applications Using the Triplex Pro 200[J]. *Journal of Thermal Spray Technology*., 2008, 17(5-6): 612-616

[14] T Y Tseng, C C Lin, J T Liaw. Phase Transformation of Gel-derived Magnesia Partially Stabilized Zirconias[J]. *Journal of Materials Science*, 1987, 22: 965-972

[15] X He, Y Z Zhang, J P Mansell, *et al.* Zirconia Toughened Alumina Ceramic Foams for Potential Bone Graft Applications: Fabrication, Bioactivation, and Cellular Responses [J]. *Journal of Materials Science*, 2008, 19: 2 743-2 749

[16] N Mesrati, Q Saif, D Treheuxb, *et al.* Characterization of Thermal Fatigue Damage of Thermal Barrier Produced by Atmospheric Plasma Spraying[J]. *Surface & Coatings Technology*, 2004, 187: 185-193

[17] H I Faraoun, T Grosdidiera, J-L Seichepine, *et al.* Improvement of Thermally Sprayed Abradable Coating by Microstructure Control[J]. *Surface & Coatings Technology*, 2006, 201: 2 303-2 312

[18] Karimi, Ch Verdon, G Barbezat. Microstructure and Hydroabrasive Wear Behaviour of High Velocity Oxy-Fuel Thermally Sprayed WC-Co(Cr) Coatings[J]. *Surface & Coatings Technology*, 1993, 57: 81-89

[19] T Patterson, A Leon, B Jayaraj, *et al.* Thermal Cyclic Lifetime and Oxidation Behavior of Air Plasma Sprayed CoNiCrAlY Bond Coats for Thermal Barrier Coatings[J]. *Surface & Coatings Technology*, 2008, 203: 437-441

[20] Y He, L Winnubst, A J Burggraaf, *et al.* Influence of Porosity on Friction and Wear of Tetragonal Zirconia Polycrystal[J]. *Journal of the American Ceramic Society*, 1977, 80(2): 377-380